# LIGHT SCATTERING AS A MEASURE OF PARTICLE SIZE IN AEROSOLS[1]

## THE PRODUCTION OF MONODISPERSE AEROSOLS

DAVID SINCLAIR[2] AND VICTOR K. LA MER

*Department of Chemistry, Columbia University, New York, New York*

*Received October 18, 1948*

### INTRODUCTION

The measurement of colloid particle size by observation of the scattered light is based primarily on the electromagnetic theory developed by Gustav Mie (16) in 1908. Previously, Rayleigh (18) had derived his well-known equations for scattering by small particles of radius much less than the wave length of the incident light. Since that time, additional investigations, both theoretical and experimental, have been made by Debye (3), Love (15), Blumer (1), Jobst (7), Engelhard and Friess (4), Ray (17), Bromwich (2), Stratton and Houghton (22), Ruedy (19), La Mer and Barnes (10), Johnson and La Mer (8), La Mer and Kenyon (12; see also 9, 11), Van de Hulst (23), and others. The complete theory is given in a compact form by Stratton (21). The pertinent equations of the Mie theory follow.

Consider a plane wave of light incident on any isotropic dielectric sphere of radius, $r$, small compared to the wave length. The total light energy scattered per second per unit intensity of illumination (unit energy per unit cross-sectional area) is:

$$S = 24\pi^3 \left| \frac{m^2 - 1}{m^2 + 2} \right|^2 \frac{V^2}{\lambda^4} \tag{1}$$

Here $V$ is the volume of the sphere equal to $4\pi r^3/3$, $\lambda$ is the wave length of the light in the surrounding medium, and $m$ is the real or complex refractive index of the particle relative to the real refractive index of the medium (see appendix A). $S$ is defined as the scattering cross-section of the sphere. Equation 1 is in the form given by Rayleigh (18) and it applies only when $r << \lambda$.

For spheres of any size the general form of equation 1 is:

$$S = \frac{\lambda^2}{2\pi} \sum_{n=1}^{\infty} (2n + 1) (|a_n|^2 + |p_n|^2) \tag{2}$$

[1] Presented at the Symposium on Aerosols which was held under the joint auspices of the Division of Physical and Inorganic Chemistry and the Division of Colloid Chemistry at the 113th National Meeting of the American Chemical Society, Chicago, Illinois, April 22, 1948.

This article is based in part on work performed for the Office of Scientific Research and Development under Contract NDRC-r33 and OEMsr-148 with Columbia University, in 1940-42. Recommendation for the contract was made by the Aerosol Section of NDRC (Dr. W. H. Rodebush, Chief) and the work was carried out under the supervision of this Section.

[2] Present address: Johns-Manville Research Center, Manville, New Jersey.

The functions $a_n$ and $p_n$ are complex functions of the parameter $\alpha = 2\pi r/\lambda$ and the index of refraction $m$. For transparent (non-absorbing) spheres $m$ is real and equation 2 yields the total amount of light abstracted (i.e., scattered) from the incident beam. For absorbing spheres $m$ is complex and equation 2 yields only that part of the light which is scattered by the sphere. (See appendices A and B for the meaning of complex index of refraction and the definitions of $a_n$ and $p_n$.)

For absorbing spheres the total light abstracted from the incident beam (i.e.,

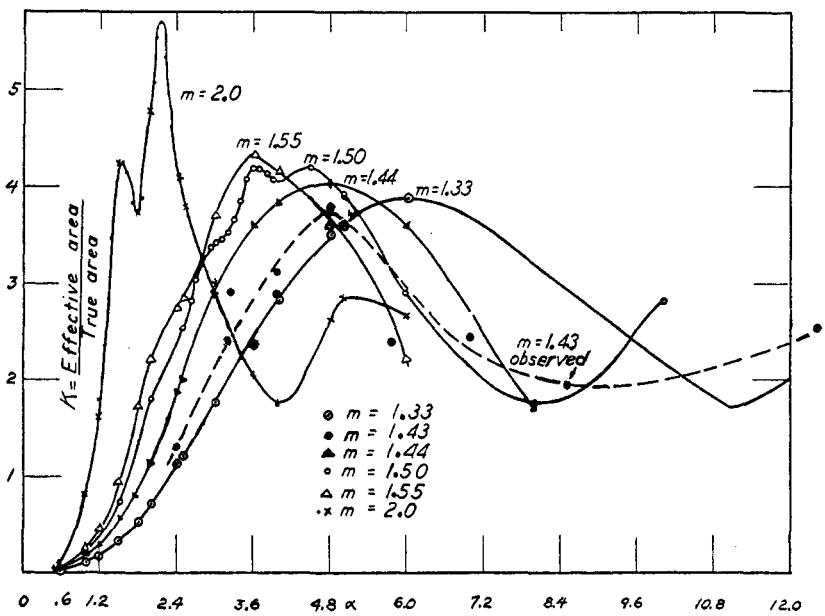


FIG. 1. Total scattering, $K_s$, per unit cross-sectional area of particle *versus* $\alpha$ (calculated). $m = 1.33, 1.44, 1.50, 1.55, 2.00$; observed $m = 1.43$.

both scattered and absorbed) per second per unit intensity of illumination is:

$$S_e = \frac{\lambda^2}{2\pi} Re\left[\sum_{n=1}^{\infty} (2n+1)\,(a_n + p_n)\right] \tag{3}$$

$S_e$ is defined as the extinction cross-section and *Re* stands for the real part of the expression in the brackets.

The sum in equation 2 has been calculated for a variety of values of $\alpha$ and $m$ (real) by The Mathematical Tables Project of the Bureau of Standards. Tables of these calculations have recently been published (14). Figure 1 shows the results obtained for five values of the real refractive index $m$. The ordinates are the "scattering area coefficient", defined as $K_s = S/\pi r^2$, i.e., the ratio of the scattering cross-section to the geometric cross-section. The abscissas are the values of $\alpha = 2\pi r/\lambda$. From equation 2 it is seen that

$$K_s = \frac{2}{\alpha^2} \sum_{n=1}^{\infty} (2n + 1) (|a_n|^2 + |p_n|^2) \tag{4}$$

so that for a given refractive index $K_s$ is a function of $\alpha$ alone.

The Mathematical Tables Project has also calculated the extinction cross-section, $S_e$, from equation 3, for a variety of absorbing particles. These calculations have not as yet been published. (See reference 8a on the scattering of ultraviolet light by sulfur hydrosols.)

The above equations hold for incident light of any state of polarization. However, the intensity scattered in a given direction varies with the state of polarization of the incident light. For example, in the limiting (Rayleigh) case when the particles are very small compared to the wave length and the *incident light is plane polarized*, the intensity scattered at an angle $\psi$ when $r < < \lambda$ is:

$$I_\psi = \frac{9\pi^2}{R^2} \left| \frac{m^2 - 1}{m^2 + 2} \right|^2 \frac{V^2}{\lambda^4} \sin^2 \psi \tag{5}$$

$R$ is the distance from the sphere to the point of observation, which must be very large compared to the radius of the sphere. $\psi$ is the angle between the direction of propagation of the scattered light and the electric vector in the incident light. The scattered light is plane polarized, with its electric vector lying in the plane defined by the electric vector in the incident light and the direction of propagation of the scattered light.

When the incident light is unpolarized, and $r < < \lambda$, the intensity scattered in the direction $\theta$ is:

$$I_\theta = \frac{9\pi^2}{2R^2} \left| \frac{m^2 - 1}{m^2 + 2} \right|^2 \frac{V^2}{\lambda^4} (1 + \cos^2 \theta) \tag{6}$$

Here $\theta$ is the angle between the directions of propagation of the incident and scattered light.

The theory predicts and observation confirms that when the incident light is unpolarized the light scattered by spheres of any size is composed of *two incoherent, plane polarized components* whose planes of polarization are mutually perpendicular. For the extremely small spheres to which equation 6 applies, the $\cos^2$ term in the parentheses gives the relative intensity of the scattered component whose electric vector lies in the plane defined by the incident beam and the observed scattered beam (hereafter referred to as the plane of observation). The term corresponding to the factor unity in the parentheses refers to the scattered component whose electric vector is perpendicular to the plane of observation. When $\theta = 90°$ it is seen that the scattered light is plane polarized with its electric vector perpendicular to the incident beam, a well-known result.

Equation 5 (but not equation 6) is in the form given by Rayleigh (18), who omitted the factor $\frac{1}{2}$ from equation 6. It should be emphasized that both equations refer to unit intensity of illumination. Our experimental and theoretical investigations have shown that the value usually given in the literature for the

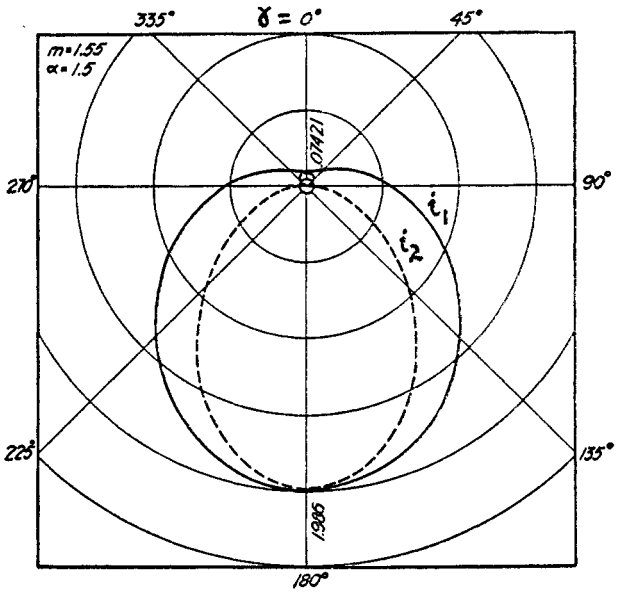


FIG. 2. Polar diagram of $i_1$ and $i_2$ for $m = 1.55$ and $\alpha = 1.5$

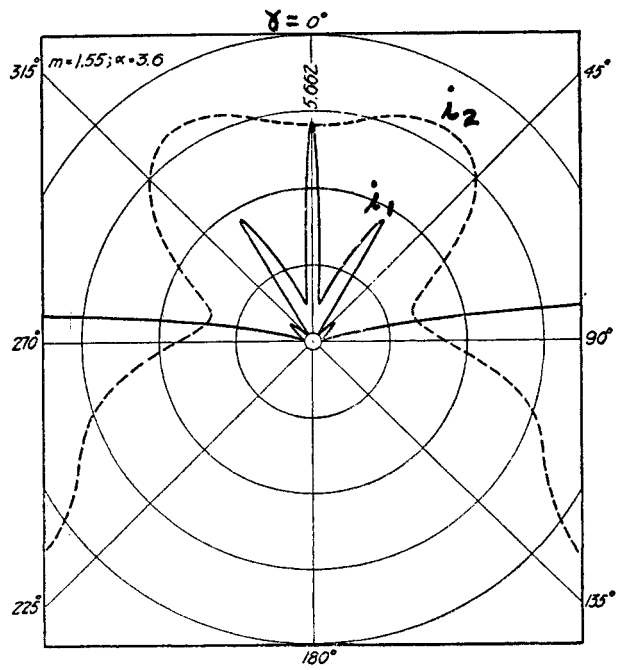


FIG. 3. Polar diagram of $i_1$ and $i_2$ for $m = 1.55$ and $\alpha = 3.6$

intensity scattered by particles illuminated by unpolarized light is too large by a factor of two, for further reasons explained elsewhere (14, 20).

For spheres of any size the general form of equation 6 should be given by Mie as:

$$I_\gamma = \frac{\lambda^2}{8\pi^2 R^2}(i_1 + i_2) \tag{7}$$

(Mie writes the factor as $\frac{1}{4}$ but it should be $\frac{1}{8}$ for the reasons given in references 14 and 20.) The angular distribution functions $i_1$ and $i_2$ are complicated functions of $\alpha$, $m$, and $\theta$. (See appendix C for definitions of $i_1$ and $i_2$.) Their values have been calculated by The Mathematical Tables Project for several values of $\alpha$ and $m$ (real), for values of $\gamma$ ($\gamma = 180° - \theta$) from 0° to 180° in steps of 10° (14). Typical results are shown in figures 2 and 3, where polar diagrams of the functions $i_1$ and $i_2$ are plotted for $m = 1.55$ and $\alpha = 1.5$ and 3.6. Similar diagrams for smaller values of $m$ are plotted in reference 1.

The functions $i_1$ and $i_2$ are proportional to the intensities of the two incoherent, plane polarized components in the scattered light. $i_1$ is the component whose electric vector is perpendicular to the plane of observation, and $i_2$ is polarized perpendicular to $i_1$. When the sphere is illuminated by unpolarized light of unit energy per unit cross-sectional area, the scattered intensity is given by equation 7. (When the incident light is plane polarized, the scattered light is elliptically polarized and $i_1$ and $i_2$ do not in general give its components.)

Theoretically the above equations can be used to measure the radius of spherical particles of any size composed of either transparent or absorbing materials. In the work described below the measurements were limited to aerosols of spherical transparent droplets, since calculations for absorbing materials were not then available. The work is further limited to radii below about 1 micron because of the practical difficulties of evaluating equations 2 and 7 for larger sizes. (Measurements of absorption in liquid sulfur sols will be found in references 8, 9, 11, and 12.) Furthermore, above 1 micron the ordinary light microscope becomes increasingly accurate and useful and accordingly the more precise methods based upon scattering become less important.

The measurements were of four types: (*1*) observation of the transmitted light as a function of wave length; (*2*) the intensity of the scattered light at a given wave length; (*3*) the color of the scattered light; (*4*) the polarization of the scattered light at a given wave length. Precise measurements were made on aerosols of uniform droplet size produced by a method described in a later section.

Measurements were also made on fogs containing a distribution of sizes. Such measurements yield an average value of the radius whose accuracy depends on the degree of uniformity of size. In many practical cases, such as the oil fog from an outdoor screening smoke generator or the aerosol required for filter penetration tests, the distribution of sizes is comparatively narrow so that the equations applicable to perfectly uniform fogs can be used with fair accuracy.

Measurements of the size distribution in non-uniform fogs were made by combining gravity settling methods with the optical methods.

The concentration was low enough so that the scattering was *incoherent* and the effect of each of the $n$ droplets per unit volume was superposed. This occurs when the ratio of droplet radius to distance of separation is about 100, corresponding to a fog of $10^6$ droplets per cubic centimeter and of radius 1 micron. The mass concentration of such a fog is about 4 mg. per liter. The mass concentration usually occurring in the laboratory and in oil fogs from an outdoor generator is a few tenths of a milligram per liter or less.

## 1. METHODS BASED ON TRANSMISSION

### *Transmission measurements*

For transparent materials the scattering cross-section, $S$ (equation 2), can be obtained by measuring the transmission as a function of wave length. Measurements at various concentrations showed that the transmission, $T$, could be expressed by the equation:

$$T = \frac{I}{I_0} = e^{-Snl} = e^{-Jcl} \tag{8}$$

Here $I_0$ is the incident and $I$ the emergent intensity of light of wave length $\lambda$, $n$ the particle number concentration, $c$ the mass concentration, $J$ the scattering cross-section per gram, and $l$ the length of path in the aerosol. When either the concentration or the radius is known, the other can be found by measuring the transmission at a known wave length. When both are unknown, they may be found by measuring the transmission at two or more wave lengths.

A beam of approximately monochromatic light from a Hilger Monochromator was passed through a uniform particle size aerosol of known concentration. The transmission was measured with a photocell, as a function of particle size and wave length, and the scattering cross-section per gram calculated from equation 8. Measurements were made at values of $T$ from about 0.9 to 0.3 for a path length of 1 m. Good agreement was obtained between the experimental values of $J$ and the theoretical values for oleic acid ($m = 1.46$), petroleum-diol ($m = 1.55$), and sulfur ($m = 2.0$). The results for oleic acid are given in figure 4. The ordinates $\lambda J$ are a function of $\alpha$ alone, and therefore valid for all radii and wave lengths, and the abscissas are log $r/\lambda$ (theoretical) and $1/\lambda$ (experimental). The curves $a$ and $b$ show the experimental results obtained for oleic acid of refractive index $m = 1.46$ and the curve to the left is the theoretical curve for $m = 1.44$. The maxima for the experimental curves occur at $\lambda J = 5.0$ cm.[3] per gram of oleic acid, in satisfactory agreement with the theoretical maximum of 5.4 cm.[3] per gram. The droplet radius determined from the horizontal displacement of the experimental maximum from the theoretical is 0.38 micron and 0.29 micron for curves $a$ and $b$, respectively, in satisfactory agreement with the

[3] The transmission method, applied to measurements on liquid sulfur hydrosols, is described in greater detail in references 8, 9, 10, 11, and 12.

observed higher-order Tyndall spectra ($3\frac{1}{2}$ and $2\frac{1}{2}$ orders, respectively) described below. The measurements on oleic acid and sulfur are described in reference 14.[3]

This method was also applied in field measurements by means of a portable photoelectric meter developed by Dr. Seymore Hochberg, called the "slope-o-meter." The relative transmission at two wave lengths through a sample of smoke gave an average particle radius, and the absolute transmission at one wave length gave the concentration.

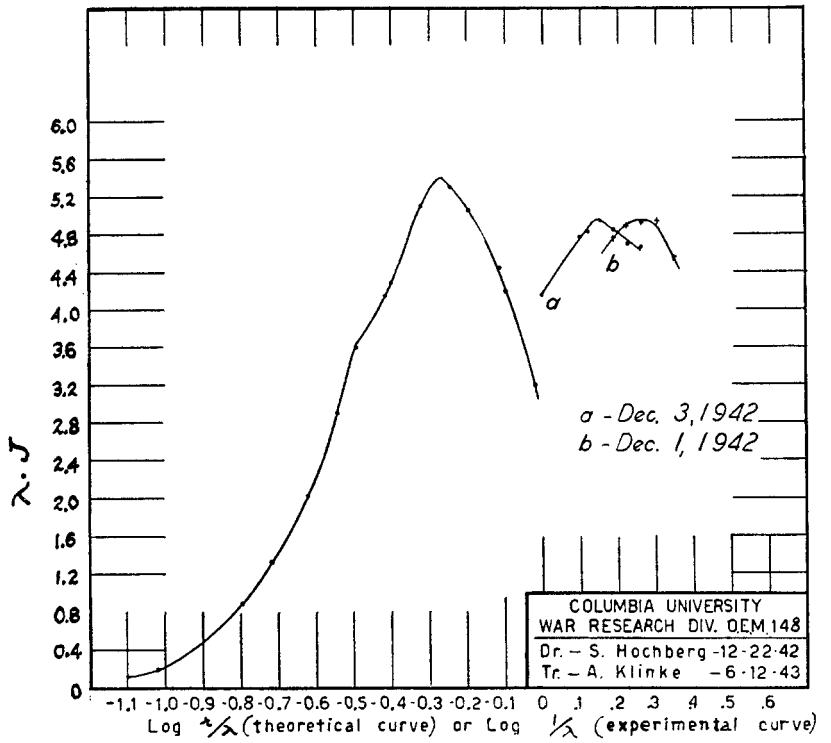


FIG. 4. Comparison of experiment with Mie theory. Oleic acid smoke. The product of wave length $\lambda$ (cm.) and scattering coefficient $J$ (cm.$^2$ per gram) as a function of radius and wave length. The experimental curves $a$ and $b$ exhibit a close approach to the theoretical value of $\lambda J = 5.4$ at the maximum.

### *Visual observations*

Visual observation of the residual color of white light transmitted through a fog provides a convenient and rapid measure of the average droplet size. Referring to the scattering coefficient $K$ in figure 1, where the abscissa $\alpha$ is proportional to $r/\lambda$, i.e., inversely proportional to wave length, it will be seen that for the values of $\alpha$ to the left of the maximum, the *scattering decreases as the wave length increases.* In other words, the transparency increases with increasing wave length. If the sun is observed through a fog whose droplet radii are smaller than the radius corresponding to the principal maximum, the sun's disc will

appear a deep red color just before extinction. *Conversely, if the radii are greater than the maximum in the K curve of figure* 1, *the residual color will be blue or green.* If the radii are grouped closely about the maximum, the residual color will be magenta. When the spread in particle size is too great, i.e., about as much as the wave length ratio of red to violet light, little or no color will be seen. This method was used to estimate the average droplet size and size distribution in the oil fogs produced outdoors. The results were in satisfactory agreement with those obtained from the photoelectric transmission meter and a portable meter (called the Owl) for scattered light described below.

## 2. METHODS BASED ON THE INTENSITY OF THE SCATTERED LIGHT

### *Absolute intensity*

The radius of the particles of a fog of uniform droplet size may be obtained by measuring the intensity scattered at angles $\theta$ varying from the forward to the backward direction and integrating over a sphere. The method is tedious and the results are not as accurate as transmission measurements.

A fog of supercooled stearic acid droplets of known uniform radius and concentration was observed while streaming out of a generator, in the form of a cylindrical jet about 1 cm. in diameter. A suitable volume was uniformly illuminated by unpolarized white light and the intensity scattered into a given small solid angle was measured with a photometer. The measurements were made through a roughly monochromatic filter ($\lambda = 0.524 \pm 0.01$ micron) at angles $\theta$ from 3° to 175°, at frequent intervals. The intensities were then integrated over a sphere and the scattering cross-section, $S$, obtained by comparison with the brightness of a diffuse reflector of known reflectivity. The results are given in the dashed curve of figure 1, in satisfactory agreement with the theoretical curve for $m = 1.44$.

The integration over the sphere of the observed scattered light when the incident light is unpolarized is mathematically equivalent to the integration of equation 7, which should be equal to equation 2. It was found, however, that the integral of equation 7 with the factor $\frac{1}{4}$ as given by Mie was equal to twice the value of $S$ given by equation 2. The satisfactory agreement between the experimental values and equation 2 shows that the absolute intensities $i_1$ and $i_2$ as originally given by Mie for equation 7 are twice too high, as mentioned above. The detailed explanation has been given elsewhere (20).

### *Relative intensity*

#### (a) Fogs of non-uniform droplet size

*At a given wave length* the observed intensity scattered at any angle, $\theta$, by particles of a given radius is directly proportional to the concentration. This is true provided the concentration is low enough so that secondary scattering is negligible. In this case the relative intensities scattered by particles of two different radii may be obtained from equation 7. For this purpose the intensities calculated from equation 7 were approximated over a small range of values of

the radius as proportional to some power of the radius. Thus the intensity, $I$, scattered in a given direction from a given volume of aerosol is proportional to the particle number concentration, $n$, and the particle radius raised to some power, i.e.,

$$I = kr^p n \tag{9}$$

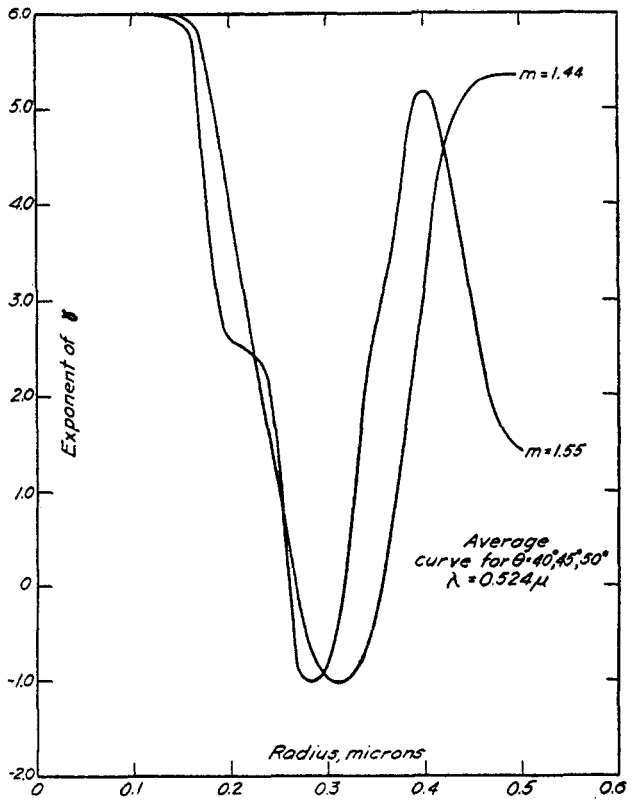


FIG. 5. Variation of $p$ with $r$ at $\theta = 40°, 45°, 50°$

The value of $p$ as a function of $r$ was obtained from the values of $(i_1 + i_2)$ given in the tables (14). The values of log $(i_1 + i_2)$ *vs.* log $r$ were plotted and the values of the slope, $p$, as a function of $r$ obtained for several angles.

Figure 5 shows the variation of $p$ with $r$ at angles $\theta = 40°$, 45°, and 50° (averaged), for refractive indices 1.44 and 1.55 at the wave length $\lambda = 0.524$ micron. It is seen that $p$ has the value 6 for radii below 0.1 micron, as is to be expected in the Rayleigh region. There is also a *region where the slope is negative*, that is, the scattering per particle actually decreases with increasing particle radius. This region, of course, corresponds to the one mentioned in the section on visual observations, where for a constant radius the *scattering increases* with increasing wave length, so that a blue transmission prevails.

The data in figure 5 may be used to obtain the size distribution in a fog of non-

uniform droplet size by allowing it to settle in a convection-free fog chamber and observing the decrease in scattered light intensity with time. The apparatus consisted of a cylindrical brass chamber $2\frac{1}{2}$ in. high and 3 in. in diameter submerged in a thermostated water bath. Fog was introduced through tubes extending down through the water bath into the fog chamber, and illuminated and observed through plane glass windows. As the fog settled, the intensity scattered by a small volume at a fixed height was measured as a function of time. The concentration of the fog was low enough so that multiple scattering and coagulation were negligible.

Consider a layer in the fog at a height $x$ below the top of the chamber, and suppose that at time $t = 0$ the concentration is uniform throughout the chamber. At the time $t_1 = x/v_1$ there will be no droplets above this layer whose velocity of fall is greater than $v_1$, and at a later time $t_2 = x/v_2$ there will be no droplets above this layer whose velocity of fall is greater than $v_2$, where $v_2$ is less than $v_1$. Consequently, observation of the decrease in number concentration at a height $x$ during the time interval $t_2 - t_1$ will give the number of particles having velocities of fall between $v_2$ and $v_1$, or radii between $r_2$ and $r_1$ given by Stokes' law of fall.

The decrease in number concentration is given by equation 9 in terms of the decrease in scattered light intensity, that is,

$$\Delta n = \Delta I / k r^p \tag{10}$$

where $r$ is now the average of the radii $r_1$ and $r_2$. The corresponding value of $p$ is obtained from figure 5. Successive measurements at different times will give the relative number of droplets of different radii.

Observations were made on an illuminated volume of fog at an angle of 45° to the incident beam. The observed volume was located a distance $x = 1.5$ cm. below the top of the chamber and the height of this volume was 2 mm. With these dimensions the intensity observed at any one time is that due to all droplets lying within the layer $1.5 \pm 0.1$ cm. from the top. This introduces an error such that a fog of uniform droplet size appears to have a spread in size of 7 per cent.

In case the law of scattering as a function of droplet size is not known for a given apparatus, it may be calibrated by observation of the intensity scattered by uniform droplet size fogs of known concentration, as described in the next section.

### (b) Fogs of uniform droplet size

When the fog is made up of droplets of uniform radius the size may be obtained by observing the rate of settling of the top of the cloud in a convection-free settling chamber. The apparatus used was similar to that described above except that the smoke chamber was a glass cylinder about 3 in. in diameter and 1 ft. high immersed in a larger glass cylinder through which water from a thermostat was circulated. The height of the cloud was recorded at suitable time intervals by sighting along the top of the cloud and recording the position on the wall of the glass water jacket.

The concentration corresponding to an observed scattered intensity was ob-

tained by passing a known volume of aerosol through a glass wool filter and weighing. The Mie theory shows that the intensity scattered at angles $\theta = 5°$ to 30° may be 100 to 1000 times that scattered at 90°. Hence, the intensity measurements were made with a new form of Tyndall meter which collected and brought to a focus all the light scattered at small angles from the forward direction. The aerosol to be collected in the glass wool filter was first passed through a cylindrical chamber 3 in. in diameter and $4\frac{1}{2}$ in. long. A small volume of the aerosol at the center of the chamber was intensely illuminated by means of a 16-cp. automobile headlight bulb. The image of the filament was formed at this point by two aspheric condenser lenses, $2\frac{1}{2}$ in. in diameter and of $2\frac{1}{4}$ in. focal length, located at one end of the chamber. The central portion of the wide angle cone of rays was blocked out by a disc $\frac{1}{2}$ in. in diameter, and the intensity of the smoke was observed through the other end of the chamber along the axis of the cone. The diameter of the observation window was slightly less than that of the blocked-out region so that no direct rays reached the photometer. An opaque screen in the center of the chamber, having an aperture just larger than the image, cut off the light scattered from the lens surfaces.

When no particles are present, the observer sees only the black background of the disc. When aerosol is passed through, the background becomes brilliantly illuminated by the light scattered at 5–30° from the direction of the incident cone of rays. The photometer is focussed on the image of the filament formed in the smoke. The brightness of this image can be measured quite accurately except when the particle size is so large and the concentration so low that flickering occurs. The sensitivity of the apparatus is such that the dust particles in the ordinary air of a room appear brilliantly illuminated. Consequently, the chamber must be air-tight and the zero reading made with well-filtered air.

This method has been further refined by Hochberg in this laboratory, and later by Gucker (5) and collaborators at Northwestern University. They measured the scattered light by using photoelectric cells in place of the visual photometer. The calibration requires the aerosols of uniform particle size which are described in the next section and are mentioned in Gucker's publication. The instrument was calibrated for smoke of a given particle size by observing the intensity at several concentrations high enough to be measured accurately by collection in the glass wool filter, but low enough so that secondary scattering and coagulation were negligible. The concentration of more dilute smokes is then directly proportional to the intensity.

This method was used for measurements of mass concentration from 200 down to $10^{-3}$ micrograms ($10^{-9}$g.) per liter, depending upon the particle size. It is believed to be the most sensitive aerosol detector ever reported. It was equalled, but not exceeded, in delicacy by the later more complicated instruments developed by Gucker and associates. For all particle sizes, the secondary scattering was negligible for concentrations of 200 micrograms per liter or less. However, coagulation sets an upper limit to the allowable mass concentration, which decreases with particle size. For example, a smoke of 0.5 micron radius will not show appreciable coagulation at concentrations up to 500 micrograms

per liter, while the concentration of a smoke of 0.15 micron radius should not be greater than 14 micrograms per liter.

### 3. METHOD BASED ON THE COLOR OF THE SCATTERED LIGHT: HIGHER-ORDER TYNDALL SPECTRA

Visual observation of the color of the light scattered at different angles by a fog of uniform droplet size provides a rapid measure of particle size. When the fog is illuminated with a parallel beam of unpolarized white light, a series of bright colors is seen as the angle of observation, $\theta$, is varied. The observation is best made through a plane polarizer oriented with its vibration direction perpendicular to the plane of observation, in which case the component $i_1$ alone is seen. The component $i_2$ exhibits a different and usually less distinct series of colors.

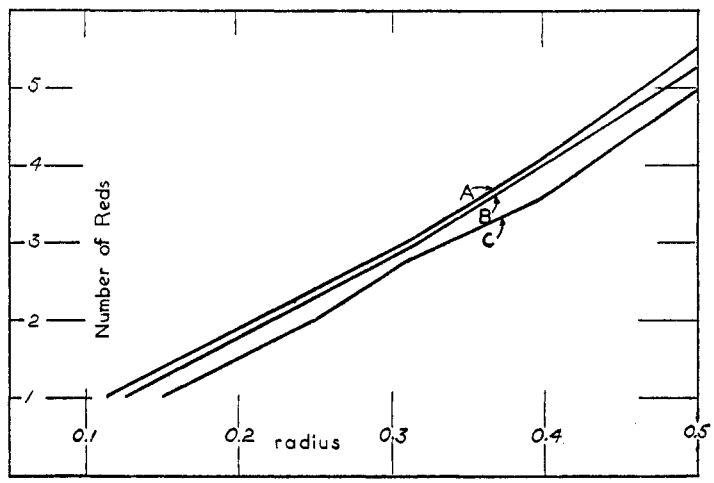


FIG. 6. Number of reds observed plotted against radius. A, sulfur (index = 2.0); B, stearic acid (index = 1.43); C, calculated (all indexes).

As the angle of observation is varied from near 0° toward 180°, the sequence of colors resembles the spectrum in the order violet, blue, green, yellow, orange, red. This spectral sequence is repeated several times depending on the particle size. Near 90° the sequence of the colors is reversed. The spectral sequences have been designated as higher-order Tyndall spectra (8), for which the Rayleigh type would be of order zero. The purity and brightness of the colors increase with uniformity of droplet size. The number of times the spectral series is repeated increases with droplet radius. The droplet radius may be measured with considerable accuracy by counting the number of times red, the most distinctive color, is seen.

Figure 6 shows the experimental curves obtained with stearic acid fogs ($m$ = 1.43) and sulfur fogs ($m$ = 2.00). The ordinates are the number of reds seen when the angle of observation is varied from near 0° to near 180°, and the abscissas are the radii in microns, obtained from measurements of the rate of settling in the convection-free chamber using Stokes' law. It is seen that the radius in

microns is roughly equal to the number of reds divided by 10. The number of reds to be expected theoretically was calculated from the values of the angular distribution function $i_1$ (equation 7) given in the tables (14). A curve was plotted for each particle radius showing the ratio of $i_1$ at $\lambda = 0.629$ micron (red) to $i_1$ at $\lambda = 0.524$ micron (green) *versus* scattering angle from 0° to 180°. The number of maxima of ratio greater than 0.45 was taken equal to the number of reds observed visually. The ratio 0.45 was chosen, since the intensity ratio at these two wave lengths is 0.9 in sunlight and 2.0 in the tungsten light used for observation. Consequently, a calculated ratio greater than 0.45 would correspond to an observed reddish hue, since the ratio in the observed scattered light

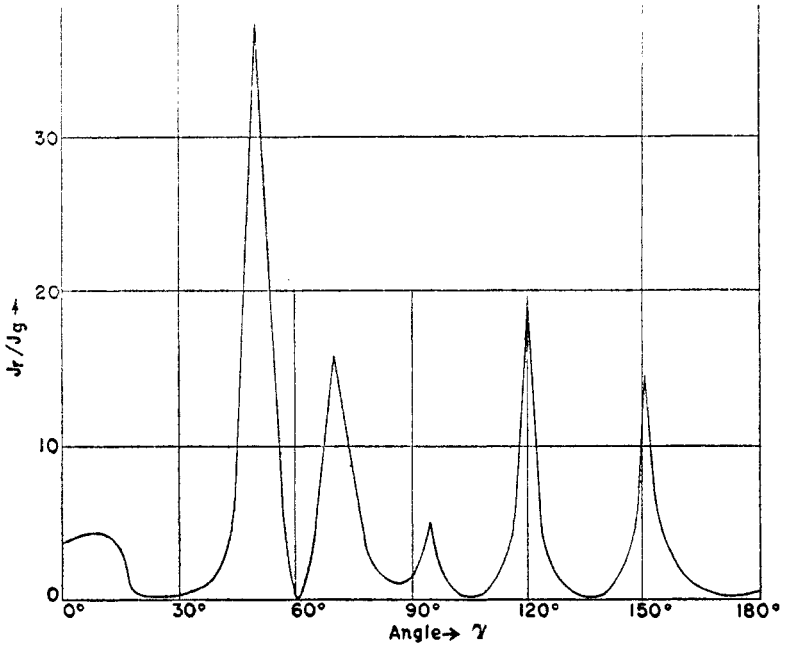


FIG. 7. Number of maxima calculated: $i_1$ (red) to $i_1$ (green) *vs.* angle $\gamma$. Red-green intensity ratio. $\alpha_r = 5$; $\lambda_r/\lambda_g = 1.2$; $m = 1.44$.

would be greater than $2 \times 0.45 = 0.9$. The tables (14) were designed to permit this calculation of the colors in scattered light by choosing successive pairs of $\alpha$-values which bear the ratio 1.2, the ratio of 0.629 to 0.524. The results are shown in curve C of figure 6. The number of maxima was found to be practically independent of refractive index throughout the range calculated from the tables. It is seen that the calculated curve differs from the experimental curves by about 0.025 micron.

Figure 7 shows the calculated red-green intensity ratio as a function of angle $\gamma = 180° - \theta$ and $m = 1.44$, corresponding to a six-order stearic acid smoke.

Figure 8 shows the angular position of the reds observed in stearic acid fogs. With the exception of sulfur the calculated points for all indices of refraction lie

on the stearic acid curves to within 5° of angle. With the aid of figure 8 greater accuracy in the particle-size measurement can be obtained by observing the angular position of the reds[4] as well as their number. The colors may be observed conveniently in a spherical flask of fog held in the hand in the parallel light beam. When the droplet size is very uniform and not larger than about 0.6 micron radius the red orders may be counted without the aid of a plane polarizer. When the droplet size is not very uniform or the radius is greater than 0.6 micron, the colors produced by the different sizes and by the two components $i_1$ and $i_2$ overlap and cause confusion. The introduction of a plane polarizer such as a disc of Polaroid between the eye and the flask gives increased clarity. No colors can be seen in fogs having a wide distribution of sizes.

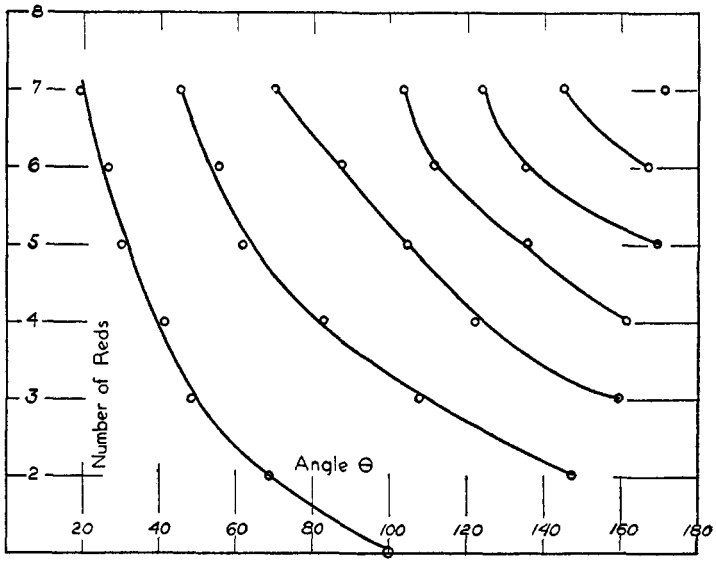


FIG. 8. Stearic acid fogs: angular position of reds observed in scattered light

When the Polaroid is held in the path of the incident light beam the observed scattered light is elliptically polarized except when the vibration direction of the Polaroid is either perpendicular or parallel to the plane of observation. With the first orientation the component $i_1$ alone and with the second orientation the component $i_2$ alone appears in the scattered light.

For accurate measurement of the angular position of the colors, the flask of fog was observed through a telescope arranged to rotate about an axis passing through the center of the flask. The light beam and telescope were directed at the center of the flask and perpendicular to the axis. The telescope carried a

[4] This method is *analogous* to the measurement of the angular position of the *coronas* observed in the light *diffracted by still larger droplets*. Humphreys (6) gives a calculated curve showing the angular radii of the first and second red coronal rings as a function of the radii of water droplets between 1 and 10 microns. It will be seen that these two curves are roughly extensions of the first two curves of figure 8.

Polaroid which could be oriented perpendicular or parallel to the plane of observation, so that the series of colors produced by either of the components $i_1$ and $i_2$ could be observed. It was found that $i_1$ gave a more distinct series of colors over a greater range of sizes.

A portable instrument (13), suitable for use either in the laboratory or in the field, was constructed for rapid measurement of the number and position of the reds. The instrument (code name "Owl") consisted of a cylindrical smoke chamber and a light source which could be held in the hand and rotated while observing the smoke through a low-power microscope. The axis of rotation was perpendicular to the plane of observation. Smoke could be drawn in and out by means of a rubber bulb and ball valves. A cylindrical window in the side of the chamber allowed observation at angles from 15° to 165° read from a graduated scale. It was found that all the reds could usually be observed in this range. The parallel beam from the light source[5] traversed the cell along a diameter and entered a tube which served as a light trap to reduce stray light. The inside of the chamber was blackened by painting and covering with soot.

The eyepiece of the microscope contained a split-field Polaroid disc of which one half had its vibration direction perpendicular and the other half parallel to the dividing line. The scattered light was observed with the dividing line perpendicular or parallel to the plane of observation, so that the component $i_1$ was seen in one half and $i_2$ in the other. The two series of colors produced by $i_1$ and $i_2$ were thus observed simultaneously but separately as the chamber and light source were rotated. This arrangement sometimes aided in estimating the size of smokes of non-uniform particle size. By placing a plane polarizer (hereafter referred to as the analyzer) between the eye and the split-field disc, the instrument was converted into a polarization photometer. In this form it was used to measure the relative intensities of the components $i_1$ and $i_2$ as described in the next section.

### 4. METHOD BASED ON THE POLARIZATION OF THE SCATTERED LIGHT

In general the relative intensity of the plane polarized components $i_1$ and $i_2$ varies in a very irregular manner with $\alpha$. However, for values of $\alpha$ below 2.5 and for angles of observation near 90°, the intensity ratio $i_2/i_1$ is a singly valued function of $\alpha$ and may be used as a measure of particle size.

The polarization photometer referred to above was used to measure the intensity ratio $i_2/i_1$ at $\lambda = 0.524$ for radii from 0.05 to 0.2 micron. A fog of uniform droplet size was observed through a Wratten green filter placed between the eye and the analyzer. With the dividing line of the split-field disc set perpendicular or parallel to the plane of observation, the analyzer was turned until the intensities of the two halves of the field were equal. If the angle between the light vibrations transmitted by the analyzer and the plane of observation is $\phi$, then:

$$i_2/i_1 = \tan^2\phi \tag{11}$$

The values of $i_1$ and $i_2$ given in the tables (14) were used to obtain theoretical

[5] Such as the Bausch & Lomb Nicholas Illuminator.

calibration curves. Figure 9 shows the calculated values of $\phi$ as a function of radius for five different refractive indices when the angle of observation $\theta = 90°$ and $\lambda = 0.524$ micron. Figure 10 shows $\phi$ as a function of radius for four values of $\phi$ when the index of refraction $m = 1.44$ and $\lambda = 0.524$ micron.

The calibration curves of figure 9 were used to measure the droplet radius of fogs of uniform size. Since the size was so small it was not possible to check the calibration curves by other experimental methods except at isolated points. Good checks were obtained for supercooled sulfur droplets of 0.11 micron radius

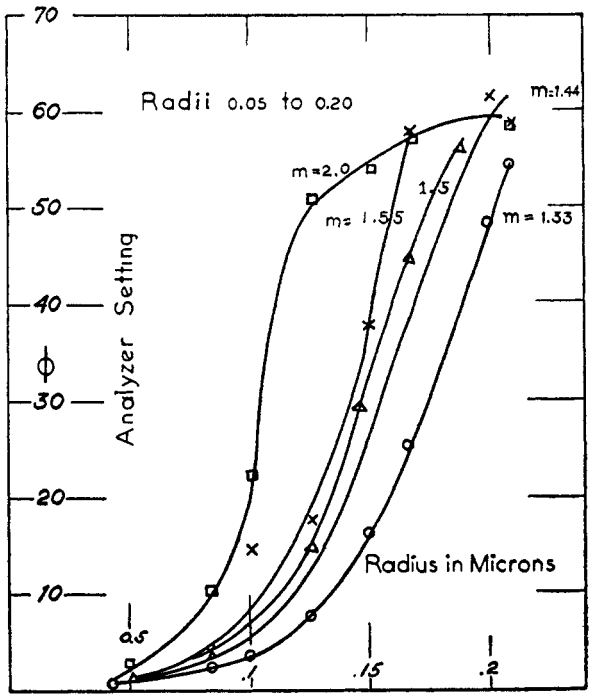


FIG. 9. Calibration curves for the Owl. Analyzer angle $\phi$ *vs.* $r$ for $\theta = 90°$ at five refractive index values.

and oleic acid droplets of 0.17 micron radius by observation of the rate of fall of uniform-sized fogs in a small, convection-free settling chamber.

Since good agreement with theory was obtained for larger sizes when using the other experimental methods described above, the polarization method is considered to be reliable for fogs of small droplet radii provided they are of sufficiently uniform size. The uniformity of size can be checked by measuring the polarization at two or more of the angles of observation given in figure 10. If the droplet radius obtained from each of these measurements is the same, then the fog is of reasonably uniform size.

It should be emphasized that the polarization method can be used only for small droplet fogs of radius below about 0.2 micron, depending upon the refractive index. In short *the method should not be used when the number of reds observed is two (2) or greater*, as the function is then not monotonic.

METHOD OF PRODUCTION OF FOGS OF UNIFORM DROPLET SIZE (13)

Stable aerosols of very uniform particle size may be produced by slow and uniform condensation of the vapors of liquids of boiling point between 300° and 500°C. when well mixed with air containing condensation nuclei. The size of the particles is determined by the ratio of the mass of condensible vapor to the number of nuclei. When the cooling and other pertinent factors are carefully controlled, it is possible to produce aerosols having a particle radius which does not vary by more than 10 per cent from the average, as shown by the direct

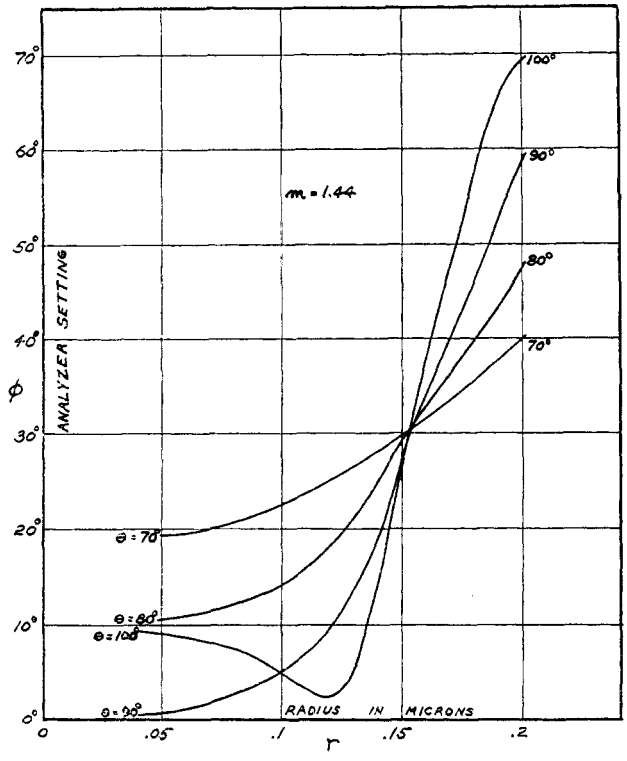


FIG. 10. Calibration curves for the Owl. Analyzer angle $\phi$ *vs.* $r$ for $m = 1.44$ at four values of $\theta$.

microscopic measurement of the droplets and the disappearance of the higher-order Tyndall spectra when aerosols of different particle radii are mixed. The reliability of this criterion of uniformity of particle size has since been tested by mixing sulfur hydrosols of uniform particle size. When sols for which the radii of the particles differed by 2 per cent were mixed, the fifth and sixth orders were obliterated (8).

The substance from which the smoke is to be formed is contained in the "boiler", a 2-l. Pyrex flask (see figure 11). The flask and contents are heated electrically in an asbestos board box to between 100°C. and 200°C. depending upon the boiling point of the substance and the particle size desired.

The condensation nuclei are formed in the "ionizer", a 1-l. Pyrex flask fitted with two electrodes sealed into standard-taper joints. The ionizer is mounted above the heater box and connected to the boiler by a standard-taper joint. The condensation nuclei may be formed by a high-voltage electric spark or an electrically heated coil of wire which has been dipped in sodium chloride. Recently (1947) it has been found by Irwin Wilson (24) that the evaporation to dryness of an aerosol produced by atomizing a dilute aqueous solution of sodium chloride in a Vaponefrin nebulizer furnishes an excellent source of radioactive sodium chloride nuclei.

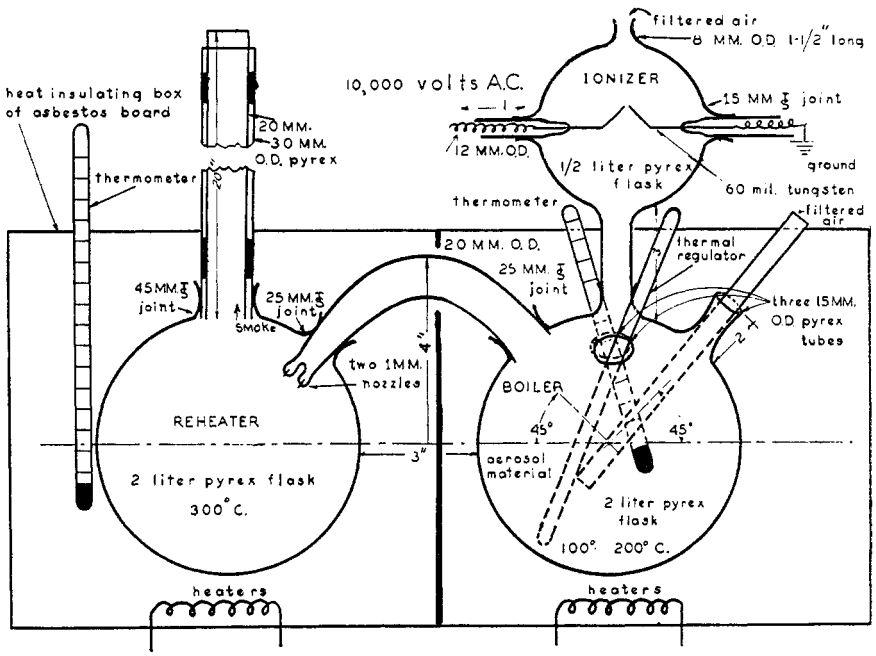


FIG. 11. Generator of aerosols of uniform particle size (improved model)

The "reheater" is a 2-l. Pyrex flask in an adjacent asbestos box heated electrically to about 300°C. A double-walled Pyrex glass chimney 20 in. long is connected to the reheater by a large standard-taper joint. The boiler and reheater are connected by a Pyrex tube having a standard-taper joint at each end. The outlet of this tube into the reheater consists of a jet having two holes of 2 mm. diameter.

A fog is produced by bubbling air through the hot liquid in the boiler, through the glass tube shown in the diagram. At the same time, air is blown in through the ionizer. The total rate of flow is usually from 1 to 4 l. per minute. The mixture of nuclei, spray, and vapor-laden air then passes through the two jet holes into the reheater. Here the spray is vaporized and the nuclei well mixed with the vapor.

The mixture then rises through the chimney, the vapor condensing uniformly

upon the condensation nuclei. The aerosol which issues from the chimney is found to be of very uniform particle size. When the column of aerosol is examined in front of a white light it is seen to be brilliantly colored, the colors varying markedly with the angle of observation.

The aerosol has mass concentration of about 1–10 mg. per liter, depending upon the particle size. In order to avoid destroying the uniformity of particle size by coagulation, the aerosol should be diluted immediately 10- or 100-fold with dry, filtered air. Small tubes or jets should not be used for this purpose, since turbulent flow destroys the uniformity of size.

The particle size is increased by increasing the temperature of the boiler, or by increasing the flow of air through the liquid relative to that through the ionizer, or by decreasing the rate of production of ions. A little practice with any given piece of apparatus will show what conditions will yield the most uniform aerosol of a given particle size.

The temperature can be maintained automatically by a thermal regulator inserted directly into the liquid or into the heater box. The air must be dried and well filtered. If it is not, the moisture, dust, and oil fog droplets in the air from a compressor or even from gas stored in a tank will provide so many condensation nuclei that the control of particle size by the ionizer will be lost.

To produce the larger particle sizes, above 1 or 2 microns radius, it is necessary to increase the proportion of vapor by bubbling the air through a porous disc. In later work (1944–45) for the production of DDT–oil aerosols of 10 microns radius for insecticidal purposes, it became necessary to invert the cooling chimney to allow the larger particles to fall out. Care must be taken to avoid decomposition of the material by excessive heating. When the walls become contaminated with decomposition products, a thorough cleaning of the apparatus improves the homogeneity of particle size.

A substance having a range of boiling points or an impurity, particularly of higher vapor pressure, is not suitable for producing a homogeneous aerosol by this method. The different components condense at different rates in the chimney, causing non-uniformity in the particle size. A volatile impurity sometimes condenses so readily that it forms sufficient nuclei to destroy the control of size by the ionizer. Fractional distillation under vacuum to avoid decomposition is often necessary for the production of sufficiently pure materials. Uniform aerosols have been produced from oleic and stearic acids, triphenyl and tricresyl phosphates, rosin, menthol, ammonium chloride, lubricating oil, and Arochlor. The convenient range of particle radius is from 0.05 to 10.0 microns. Smaller sizes may be produced, but it is difficult to measure the size or uniformity.

In general, the larger particle aerosols are relatively more uniform in size. The result arises from the law of growth, which is of the form $r = \sqrt{r_0^2 + kt}$ (24, 25). Here $k$ is a constant depending upon degree of supersaturation and diffusion rate, $r_0$ is the radius of the nucleus, and $r$ is the radius produced after a time $t$. For example, with $kt = 0.16$ micron, an initial nucleus of $r_0 = 0.01$ micron yields an $r$ value of 0.40 micron, whereas with a nucleus of $r_0 = 0.1\ \mu$, $r = \sqrt{0.17} = 0.41\ \mu$. With large values of $kt$ relative to $r_0^2$ any initial variations in $r_0$

are obliterated. Running the generator with and without condensation nuclei has a very pronounced effect on the uniformity of particle size. The nuclei may be ionized air molecules or molecules of such substances as nitrogen dioxide, hydrogen, oxygen, or ammonia. When a too intense, flaming spark is used, nitrogen dioxide is readily detectable by its odor and color.

## REFERENCES


(1) BLUMER, HANS: Z. Physik **32**, 119 (1925); **38**, 304, 920 (1926); **39**, 195 (1926).
(2) BROMWICH, T. J.: Phil. Trans. **220A**, 189 (1920).
(3) DEBYE, P.: Ann. Physik **30**, 57 (1909).
(4) ENGELHARD, H., AND FRIESS, H.: Kolloid-Z. **81**, 129 (1937).
(5) GUCKER, F. T., SR., PICKARD, H. B., AND O'KONSKI, C. T.: J. Am. Chem. Soc. **69**, 429 and 2422 (with J. N. Potts) (1947).
(6) HUMPHREYS, W. J.: *Physics of the Air*, p. 554. McGraw-Hill Book Company, Inc., New York (1940).
(7) JOBST, G.: Ann. Physik **76**, 863 (1925).
(8) JOHNSON, I., AND LA MER, V. K.: J. Am. Chem. Soc. **69**, 1184 (1947).
(8a) KENYON, A. S., AND LA MER, V. K.: J. Colloid Sci. **3**, 163 (1949).
(9) LA MER, V. K.: J. Phys. Colloid Chem. **52**, 95 (1948).
(10) LA MER, V. K., AND BARNES, M. D.: J. Colloid Sci. **1**, 71, 79 (1946).
(11) LA MER, V. K., BARNES, M. D., KENYON, A. S., AND ZAISER, E. M.: J. Colloid Sci. **2**, 349 (1947).
(12) LA MER, V. K., AND KENYON, A. S.: J. Colloid Sci. **2**, 257 (1947).
(13) LA MER, V. K., AND SINCLAIR, D.: "Portable Optical Instrument for Measurement of Particle Size in Smokes"; "An Improved Homogeneous Aerosol Generator," Report No. 32200, Office of Publications Board, Department of Commerce, and OSRD Report No. 1668.
(14) LA MER, V. K., AND SINCLAIR, D.: "Verification of Mie Theory," OSRD Report No. 1857 and Report No. 944, Office of Publications Board, U. S. Department of Commerce; to appear also as a special publication of the Bureau of Standards Applied Mathematical Computations.
(15) LOVE, A. E. H.: Proc. London Math. Soc. **30**, 308 (1899); **31**, 489 (1899).
(16) MIE, G.: Ann. Physik **25**, 377 (1908).
(17) RAY, B.: Proc. Indian Assoc. Cultivation Sci. **7**, 1 (1921).
(18) RAYLEIGH, LORD: *Scientific Papers*, Vol. I, pp. 92–3; Vol. IV, p. 400. Cambridge University Press, London (1899).
(19) RUEDY, R.: Can. J. Research **19A**, 117 (1941); **21A**, 79, 99 (1943); **22A**, 53 (1944).
(20) SINCLAIR, D.: J. Optical Soc. Am. 37, 475 (1947).
(21) STRATTON, J. A.: *Electromagnetic Theory*, p. 563. McGraw-Hill Book Company, Inc., New York (1941).
(22) STRATTON, J. A., AND HOUGHTON, H. G.: Phys. Rev. **38**, 159 (1931).
(23) VAN DE HULST, H. C.: *Optics of Spherical Particles.* Duwaer & Sons, Amsterdam, Netherlands (1946).
(24) WILSON, I., AND LA MER, V. K.: J. Ind. Hyg. Toxicol. **30**, 265 (Sept. 1948).
(25) ZAISER, E. M., AND LA MER, V. K.: J. Colloid Sci. **3**, 571 (December, 1948).


## APPENDIX A

### *Absorbing media*

Absorption may arise from two causes: (*1*) in conducting media for which the conductivity, $\sigma$, is finite, and (*2*) in dielectrics when the incident wave length is not far from that of an emission line. The first type of absorption is the only one

considered in the derivation of the Mie theory. The second type of absorption results from the interaction of bound electrons and the incident electromagnetic wave. The details of the derivation are outside the scope of this paper. As indicated below, this type of absorption may be measured and used in the calculation of light scattering by spherical particles in the same manner as the absorption arising from conduction.

The notion of a complex refractive index is useful whenever absorption occurs. This can be seen by comparing the solutions of the electromagnetic wave equation for transparent and absorbing (conducting) media for which the magnetic permeability is unity. For example, the solution of a plane polarized wave propagated in the $+z$ direction is:

$$E_0 e^{iwt} e^{-ipz}$$

where $E_0$ is the amplitude of the electric vector, $w$ is the angular frequency, $p$ is the propagation constant, and $i = \sqrt{-1}$. In transparent media $p$ has the value $2\pi m/\lambda$, where $\lambda$ is the wave length in free space and $m$ is the real refractive index.

In conducting media, owing to the conduction of free electrons, $p$ has the value:

$$\sqrt{\frac{4\pi^2 m^2}{\lambda^2} - \frac{8\pi^2 \sigma}{c\lambda} i}$$

where $c$ is the velocity of light in free space.

By analogy with transparent media the complex quantity, $p$, when multiplied by $\lambda/2\pi$, yields the complex refractive index:

$$m_c = p\frac{\lambda}{2\pi} = \sqrt{m^2 - \frac{2\sigma}{\nu} i}$$

where $m$ is the real part of the refractive index and $\nu$ is the frequency. If now we write:

$$m_c = m(1 - ik)$$

the solution of the wave equation may be expressed in terms which are readily measurable experimentally. Thus:

$$p = \frac{2\pi}{\lambda} m(1 - ik)$$

so that the solution becomes:

$$E_0 e^{-2\pi mk/\lambda} z e^{i[wt-(2\pi mz/\lambda)]}$$

an exponentially damped wave. Since the intensity is proportional to the square of the amplitude, the absorption coefficient, $\mu$, will be given by:

$$\mu = \frac{4\pi k}{\lambda}$$

i.e., the intensity of a plane wave decreases to the fraction $l^{-4\pi kl/\lambda}$ of its original value when the light passes through a distance $l$ of the substance. The quantity,

$k$, is called the absorption index. It is commonly determined by measurement of the absorption coefficient, $\mu$, in the bulk material at a given wave length. Similarly, the real part of the refractive index, $m$, must be determined for each wave length, particularly for highly absorbing media, in which $m$ varies rapidly with wave length.

In the case of absorption of wave lengths near an emission line of a dielectric the absorption index, $k$, and the real refractive index, $m$, may be measured in the same manner. In either case the complex refractive index $m(1 - ik)$ when substituted in equation 1 or 2 gives the light scattered, i.e., exclusive of that absorbed, by absorbing particles. When $m(1 - ik)$ is used in equation 3, one obtains both the scattered and the absorbed light. Any of the equations 1 to 7 can be used with either a real or a complex refractive index, depending on the nature of the aerosol and the quantity desired.

## APPENDIX B

At the request of the referee we give definitions and meanings of $a_n$ and $p_n$. In the solution of the Maxwell equations, as given by Mie (1908), Debye (1909), and Rayleigh (1911), both the incident wave and the scattered wave are developed into electric and magnetic multipole components. Since the scattered components are coherent, they will interfere. Interference of the scattered wave with the incident wave produces extinction. Mutual interference among the components of the scattered wave determines the intensity of the scattered light. Each electric or magnetic multipole component is characterized by a coefficient. Thus for the $2^n$ electric component:

$$a_n = \frac{\alpha\psi'_n(\beta)\psi_n(\alpha) - \beta\psi'_n(\alpha)\psi_n(\beta)}{\alpha\psi'_n(\beta)\zeta_n(\alpha) - \beta\zeta'_n(\alpha)\psi_n(\beta)}$$

and for the $2^n$ magnetic component:

$$p_n = \frac{\alpha\psi_n(\beta)\psi'_n(\alpha) - \beta\psi_n(\alpha)\psi'_n(\beta)}{\alpha\psi_n(\beta)\zeta'_n(\alpha) - \beta\zeta_n(\alpha)\psi'_n(\beta)}$$

Here $\alpha = 2\pi r/\lambda$ and $\beta = m\alpha$.

The cylindrical functions appearing above are defined as

$$\psi_n(\alpha) = \left(\frac{\pi\alpha}{2}\right)^{1/2} J_{n+\frac{1}{2}}(\alpha); \qquad \chi_n(\alpha) = (-1)^n \left(\frac{\pi\alpha}{2}\right)^{1/2} J_{-n-\frac{1}{2}}(\alpha)$$

and

$$\zeta_n(\alpha) = \psi_n(\alpha) + i\chi_n(\alpha)$$

Primes denote derivatives and $J$ represents a Bessel function of half order. In studying the theory the reader will encounter spherical harmonics defined as:

$$\pi_n(v) = \frac{1}{\sin\theta} P^1_n(v) \quad \text{and} \quad \tau_n(v) = \frac{\mathrm{d}}{\mathrm{d}\theta} P^1_n(v)$$

both derived from $P^1_n(v)$, the first associated Legendre function with $v = \cos\theta$,

with the additional useful relation

$$\tau_n(v) = v\pi_n(v) - (1 - v^2)\pi_n^1(v) = \operatorname{cotg}\theta\, P_n^1(v) - P_n^2(v)$$

The functions $\psi_n(\alpha)$ and $\chi_n(\alpha)$ are real when their arguments are real. Both $\alpha$ and $\beta$ are real if the refractive index $m$ is real, as holds for dielectric spheres. The case of totally reflecting spheres, having $m$ = infinity, may be included.

The cylindric functions behave differently for small and large values of the argument. Thus:

Small $\alpha$:

$$\psi_n(\alpha) = \frac{\alpha^{n+1}}{1\cdot 3\cdots(2n+1)}; \quad \chi_n(\alpha) = \frac{1\cdot 3\cdots(2n+1)}{\alpha^n}$$

represents the first term of a convergent series practicable for $\alpha << n$.

Large $\alpha$:

$$\psi_n(\alpha) = \sin\left(\alpha - \frac{n\pi}{2}\right); \qquad \chi_n(\alpha) = \cos\left(\alpha - \frac{n\pi}{2}\right)$$

shows the first term of a semiconvergent series practicable when $\alpha >> n$. Debye (1909) has derived semiconvergent developments for intermediate values of $\alpha$ and $n$, which connect the above formulas, useful when both $\alpha$ and $n$ are large. The computations of the tables by Lowan and associates are based upon the above definitions. The reader should refer to the excellent dissertation of van de Hulst (23) for more details of the meaning of the equations and for improvements in computational schemes, particularly Chapters 2 and 9. In his notation our $\alpha = x$ and our $\beta = y$ (see also Stratton (21)).

## APPENDIX C

### *Definition of $i_1$ and $i_2$ in equation 7*

The definitions of $i_1$ and $i_2$ are obtained from the equations and definitions in appendix B by calculating the energy flux by means of the Poynting vector in the limit for an observer at an infinite distance from the sphere, i.e., $R >> r$.

$$i_1(\theta) = \left| \sum_{n=1}^{\infty} \frac{2n+1}{n(n+1)} \{a_n\pi_n(v) + p_n\tau_n(v)\} \right|^2$$

$$i_2(\theta) = \left| \sum_{n=1}^{\infty} \frac{2n+1}{n(n+1)} \{p_n\pi_n(v) + a_n\tau_n(v)\} \right|^2$$

In the van de Hulst reference (23, p. 8), compact formulae are also given for computing the total amount of scattered light and the total forward component by the use of the integrals of products of the functions $\pi_n(v)$ and $\tau_n(v)$ on the sphere as derived originally by Debye.